To be presented at the 32nd U.S. Symposium on Rock Mechanics, July 10-12, 1991, in Norman, Oklahoma.

SAND90-2399C

The closure of WIPP disposal rooms filled with various waste and backfill combinations[1]

SAND--90-2399C

DE91 008187

J. Randall Weatherby, William T. Brown, Barry M. Butcher
Sandia National Laboratories, Albuquerque, New Mexico, USA

ABSTRACT: Two-dimensional finite element analyses were used to investigate the closure of WIPP disposal rooms filled with backfill and rooms filled with a combination of waste and backfill. Two different backfill materials were considered. The analyses provide estimates of the porosity in the disposal room as a function of time. These results have been used to help evaluate the suitability of the backfill materials for use in the repository.

1 INTRODUCTION

The Waste Isolation Pilot Plant (WIPP) located near Carlsbad, New Mexico is being developed by the U. S. Department of Energy for the purpose of providing a research and development facility to demonstrate the safe disposal of transuranic waste resulting from defense activities. The facility will consist of an array of rooms mined in a bedded salt formation at a depth of 650 meters below ground level. Under the present design, the majority of the contact-handled transuranic (CH-TRU) waste will be stored in a loosely-packed state inside of 55-gallon drums. Backfill will then be placed in the empty space surrounding the drums and in the access-ways to the disposal rooms.

Because the salt formation is a creeping medium, each disposal room will close over time compacting the waste and backfill. As a result of this compaction, both the waste and backfill will become much less permeable to the flow of brine than they are initially. The room closure will also slow and eventually stop as the stresses increase in the material inside of the room and thus apply a back pressure to the room boundary.

Placing backfill in the rooms and access-ways reduces the initial amount of void volume in the repository and thereby decreases the length of time required to sufficiently compact the waste. The use of backfill also decreases the amount of damage that will accumulate in the salt formation by reducing the amount of closure required to reach the final compacted state. Additives can be included in the backfill to absorb brine, gas, and radionuclides.

One backfill material under consideration is crushed salt. The desirable characteristics of the crushed salt are: (1) it is readily available, and (2) it is physically and chemically

[1]This work supported by the United States Department of Energy (DOE) under Contract No. DE-AC04-76DP00789.

compatible with the salt formation that surrounds the repository. The second backfill that has been considered is a mixture consisting of crushed salt and bentonite. The major advantage of including bentonite in the backfill is its ability to absorb both water and radionuclides. A disadvantage is that salt/bentonite mixtures are slower to consolidate under pressure than an all-salt backfill. This disadvantage is offset to some extent by the fact that salt/bentonite mixtures have a lower permeability for a given porosity than an all-salt backfill.

Four different disposal room configurations have been analyzed using the two-dimensional finite element code SANCHO (Stone, et al. 1986). The disposal room geometry was the same in each configuration, only the contents of the room were varied. The following conditions were analyzed: (1) a room completely filled with an all-salt backfill, (2) a room completely filled with a salt-bentonite mixture containing 70% by weight crushed salt and 30% by weight bentonite, (3) a room containing waste surrounded by an all-salt backfill, and (4) a room containing waste surrounded by a 70% salt 30% bentonite backfill. The main objective behind this work was to produce estimates of the porosity in the waste and backfill as functions of time. This information can be used as a basis for selecting a suitable backfill. The results can also be used to help determine if some form of preprocessing will be necessary to reduce the initial porosity in the waste containers.

2 GEOMECHANICAL FINITE ELEMENT MODEL

In all four cases, the geometric idealization in Figure 1 was used to model the disposal room and its contents. Because of symmetry, only the upper right quadrant of the configuration in Figure 1 was actually modeled. The salt formation and the contents of the room were assumed to be in a state a plane strain. In the two cases where both waste and backfill were present in the disposal room, the backfill region surrounded the waste region as shown in Figure 1. In the two remaining cases, all elements inside of the room were assumed to be backfill (including those in the region labeled "waste" in Figure 1).

The boundary conditions applied in the analysis simulate the conditions that would exist around a deeply buried disposal room located near the middle of a long panel of equally spaced disposal rooms. The right boundary of the modeled region represents the centerline between two disposal rooms, while the left boundary of the mesh represents the centerline of the disposal room. Both of these boundaries were fixed against horizontal motion based on symmetry conditions. The lower boundary of the mesh, which passes through the midheight of the disposal room, was fixed against vertical motion. A pressure of 14.8 MPa was applied along the upper boundary, and all locations in the salt formation were given an initial stress state with all three principal stresses set equal to -14.8 MPa. This corresponds to the undisturbed lithostatic stress state that is believed to exist at the repository horizon. The weight of the room contents and the intact salt in the modeled region were not considered because they have little effect on the deformation of the room (Arguello 1989).

3 CONSTITUTIVE MODELS

The intact salt was modeled with the elastic/secondary creep relation described in Krieg (1984). In this model, the relationship between the mean stress and the true volumetric strain is linear elastic. Inelastic terms appear in the relationship between the deviatoric stress and deviatoric strain. The elastic bulk and shear moduli used for the intact salt were obtained by dividing the measured values by a factor of 12.5. This artificial reduction in the elastic moduli produced good agreement between computed and in-situ closures (Morgan and Krieg 1988) when an all-salt stratigraphy was used to model the salt formation.

The backfill consolidates as a function of time under both constant and time-varying compressive stresses. Creep consolidation experiments have been conducted under various pressure levels for both an all-salt backfill (Holcomb and Shields 1987) and a 70% crushed salt, 30% bentonite backfill (Pfeifle 1991). An empirical constitutive model was developed from the creep consolidation tests on salt backfill (Sjaardema and Krieg 1987). This constitutive model accounts for both volumetric and deviatoric creep. The model has been implemented in the two-dimensional finite element code SANCHO (Stone, et al. 1986). A brief description of the backfill model is given below.

In order to describe the constitutive relations for the backfill, several quantities must first be defined. The Cauchy stress tensor is denoted by σ_{ij}, and the velocity vector is denoted by v_i. The stretching tensor d_{ij} and the spin tensor w_{ij} are defined as:

$$d_{ij} = \frac{1}{2}(v_{i,j} + v_{j,i}) \quad (1)$$

$$w_{ij} = \frac{1}{2}(v_{i,j} - v_{j,i}) \ . \quad (2)$$

Both the Cauchy stress tensor and the stretching tensor can be decomposed into spherical and deviatoric parts through:

$$\sigma_{ij} = s_{ij} - \delta_{ij}p \quad (3)$$

$$d_{ij} = d'_{ij} - \frac{1}{3}\delta_{ij}\dot{e}_v \quad (4)$$

where s_{ij} and d'_{ij} are the deviatoric parts of the Cauchy stress tensor and stretching tensor, respectively, and

$$p \equiv -\frac{1}{3}\sigma_{kk} \quad (5)$$

$$\dot{e}_v \equiv -d_{kk} \ . \quad (6)$$

The corotational flux of the Cauchy stress tensor is defined to be:

$$\overset{\triangledown}{\sigma}_{ij} = \dot{\sigma}_{ij} - w_{ik}\sigma_{kj} + \sigma_{ik}w_{kj} \quad (7)$$

where $(\dot{\ })$ refers to the derivative with respect to time. The following relationship between the corotational flux of the Cauchy stress, the corotational flux of the deviatoric stress $\overset{\triangledown}{s}_{ij}$, and the hydrostatic pressure p can be shown to hold:

$$\overset{\triangledown}{\sigma}_{ij} = \overset{\triangledown}{s}_{ij} - \delta_{ij}\dot{p} \ . \quad (8)$$

In the backfill constitutive model, the rate of dilatation $\dot{e}_v$ is assumed to depend on the hydrostatic pressure p through:

$$\dot{e}_v = \dot{p}/K + \frac{1}{\rho}B_0\left[e^{B_1 p} - 1\right]e^{A\rho} \quad (9)$$

where B_0, B_1, and A are the material constants obtained from the creep consolidation experiments, K is the elastic bulk modulus, and ρ is the density of the backfill. The density ρ is computed from the relationship:

$$\rho = \rho_0 \exp\left(\int_{t_0}^{t} \dot{e}_v \, dt\right) \tag{10}$$

where ρ_0 is the density at time t_0.

The deviatoric part of the stretching tensor is assumed to depend on the deviatoric stress and corotational flux of the deviatoric stress through the relationship (Sjaardema and Krieg 1987):

$$d'_{ij} = \frac{\overset{\nabla}{s}_{ij}}{2G} + \frac{3}{2}A_c\left(\frac{\rho_{\text{intact}}}{\rho}\right)^N \exp(Q/RT)\,(1.5 s_{kl}s_{kl})^{(N-1)/2} s_{ij} \tag{11}$$

where A_c, N, and Q are material constants obtained from uniaxial creep experiments on intact salt, R is the ideal gas constant, T is the absolute temperature, G is the elastic shear modulus, and ρ_{intact} is the density of the intact salt.

The elastic moduli are assumed to depend on the density of the backfill through relationships of the form:

$$K = K_0 \exp(K_1 \rho) \tag{12}$$

$$G = G_0 \exp(G_1 \rho) \tag{13}$$

The empirical equation for the elastic bulk modulus K is based on data from a hydrostatic test on dry crushed salt (Holcomb and Hannum 1982). In this experiment, the bulk modulus was determined by performing unload-reload cycles on the same specimen at different degrees of consolidation. Constants K_0 and K_1 were determined by using the least squares method to fit the modulus data to the function in Equation 12 (Sjaardema and Krieg 1987). In the fit, the function was constrained so that the bulk modulus of the crushed salt was equal to the bulk modulus of the intact salt when the crushed salt was fully compacted. No experiments have been conducted to determine how the shear modulus varies with density, so the shear modulus was assumed to vary according to the same exponential form as the bulk modulus. The constant G_0 was selected so that the shear modulus for the crushed salt was equal to that of the intact salt when the crushed salt was fully consolidated, and the constant G_1 was assumed to be the same as K_1. Because the shear and bulk moduli of the intact salt were divided by 12.5, G_0 and K_0 were divided by the same factor. A parametric study has shown that the results are relatively insensitive to the values of K_0 and G_0. Table 1 lists the values of the creep constants and elastic constants used for the two different backfill materials.

The stress-strain behavior of the waste was represented by a volumetric plasticity model with a piecewise linear function defining the relationship between the mean stress p and the volumetric strain e_v. Compaction experiments on simulated waste were used to develop this relationship. Table 2 lists the ordered pairs that define the piecewise linear relationship between p and e_v in the two analyses that include waste.

The deviatoric response of the waste material has not been characterized. It is anticipated, however, that when a drum filled with loosely compacted waste is compressed axially, the drum will not undergo significant lateral expansion until most of the void space inside the drum has been eliminated. The constants in the volumetric plasticity model were defined to capture this anticipated characteristic. The deviatoric yield function F for the waste has the form:

$$F = \bar{\sigma} - 3p = 0 \tag{14}$$

Table 1: Constants Used With the Backfill Model for the All-Salt and Salt/Bentonite Backfills.

Parameter	Value	
	All-Salt	Salt/Bentonite
A_c ($Pa^{-4.9}$/(sec.))	5.79×10^{-36}	5.79×10^{-36}
N	4.9	4.9
Q/RT	20.13	20.13
A (m^3/kg)	-17.3×10^{-3}	-34.5×10^{-3}
B_0 (kg/(m^3 sec))	1.3×10^{8}	1×10^{21}
B_1 (Pa^{-1})	0.82×10^{-6}	0.6×10^{-6}
K_0 (Pa)	1408.	1408.
G_0 (Pa)	848.	848.
K_1,G_1 (Pa)	0.00653	0.00653

Table 2: Assumed relationship between the mean stress and the volume strain for the CH-TRU waste.

Mean Stress, p (MPa)	Volume Strain, e_v ($\log(\rho/\rho_0)$)
0.028	0.032
0.733	0.741
1.133	0.898
1.667	1.029
2.800	1.180
10.17	1.536

where $\bar{\sigma} = \sqrt{\frac{3}{2} s_{ij} s_{ij}}$. The deviatoric response was assumed to be elastic-perfectly plastic. The values assumed for the elastic shear modulus and elastic bulk modulus were 222 (MPa) and 333 (MPa), respectively. A non-associative flow rule was used so that the plastic part of the deviatoric stretching tensor was given by:

$$(d'_{ij})^p = \dot{\lambda} s_{ij} \ . \tag{15}$$

5 FINITE ELEMENT RESULTS

The closure of the disposal room was simulated for the first 200 years following excavation for the two cases where the room contained only backfill, and for the first 800 years following excavation for the two cases where the room contained both waste and backfill. Time was advanced in 0.025 year increments. The problem was defined so that the elastic closure of the room at the time of excavation did not produce stresses in the waste or backfill.

Figure 2 shows the computed change in width of the disposal room (expressed as a percentage of the initial width of the room) as a function of time for the four cases that were analyzed. Similar plots contained in Figure 3 show the change in height measured between the center of the ceiling and the center of the floor as a function of time for each of the four cases. In all cases, the room contents were crushed to a greater extent in the vertical direction than in the horizontal direction. More closure was observed in the rooms containing both waste and backfill as compared to the rooms containing only backfill because the waste had a much greater initial porosity than the backfill. Figures 2 and 3 show that the salt/bentonite backfill slows the closure of the room in comparison to the closure of rooms containing all-salt backfill.

At time t, the average porosity P for any region in the disposal room can be computed from the relationship:

$$P(t) = \frac{1}{V(t)} \int_V (1 - \rho(t)/\rho_{\text{intact}}) \, dV \tag{16}$$

where $V(t)$ is the volume of the region at time t. This relationship assumes that the porosity goes to zero as the density of the backfill approaches the density of the intact salt. Figure 4 shows how the average porosity in the backfill decreased as a function of time for the two cases with all-salt backfill. In both cases, the average porosity in the backfill decreased to 5% thirty years after excavation and emplacement of the room contents. The two plots in Figure 5 show how the average backfill porosity changed as a function of time for the two cases where salt-bentonite backfill was used. These results demonstrate that the salt-bentonite mixture consolidated at a much slower rate than the all-salt backfill. For the two cases where salt-bentonite was used, 9% porosity still remained in the salt-bentonite backfill after 200 years of closure. The reduction in porosity in the waste is shown in Figure 6 for the case with all-salt backfill and for the case with salt-bentonite backfill. Because the initial volume of the waste is so much larger than the initial volume of the backfill, the rate of waste compaction was virtually the same for both cases.

6 SUMMARY AND CONCLUSIONS

The results of the finite element analyses show the degree to which bentonite slows the consolidation of crushed-salt backfill in a disposal room as compared to an all-salt backfill. The average porosity in the all-salt backfill decreased to less than 5% within the first 35 years after excavation, while approximately 10% porosity remained in the salt-bentonite backfill 200 years after excavation. The results also indicate that the slower consolidation of the salt-bentonite backfill will not significantly affect the rate of waste compaction.

REFERENCES

Argüello, J. G. 1990. Use of midheight symmetry plane to compute disposal room closure. Sandia memorandum, Sandia National Laboratories, Albuquerque, NM.

Holcomb, D. J. & D. W. Hannum 1982. Consolidation of crushed salt backfill under conditions appropriate to the WIPP facility. SAND82-0630. Sandia National Laboratories, Albuquerque, NM.

Holcomb, D. J. & M. Shields 1987. Hydrostatic creep consolidation of crushed salt with added water. SAND87-1990. Sandia National Laboratories, Albuquerque, NM.

Krieg, R. D. 1984. Reference stratigraphy and rock properties for the Waste Isolation Pilot Plant (WIPP) project. SAND83-1908. Sandia National Laboratories, Albuquerque, NM.

Morgan, H. S. & R. D. Krieg 1988. A comparison of unified creep-plasticity and conventional creep models for rock salt based on predictions of creep behavior measured in several in situ and bench-scale experiments. SAND87-1867. Sandia National Laboratories, Albuquerque, NM.

Pfeifle, T. W. 1991. Consolidation, permeability, and strength of crushed salt/bentonite mixtures with application to the WIPP. SAND90-7009. Sandia National Laboratories, Albuquerque, NM.

Sjaardema, G. D. and R. D. Krieg 1987. A constitutive model for the consolidation of WIPP crushed salt and its use in analyses of backfilled shaft and drift configurations. SAND87-1977. Sandia National Laboratories, Albuquerque, NM.

Stone, C. M., R. D. Krieg, & Z. E. Beisinger 1985. SANCHO, a finite element code for the quasistatic, large deformation, inelastic response of two-dimensional solids. SAND84-2618. Sandia National Laboratories, Albuquerque, NM.

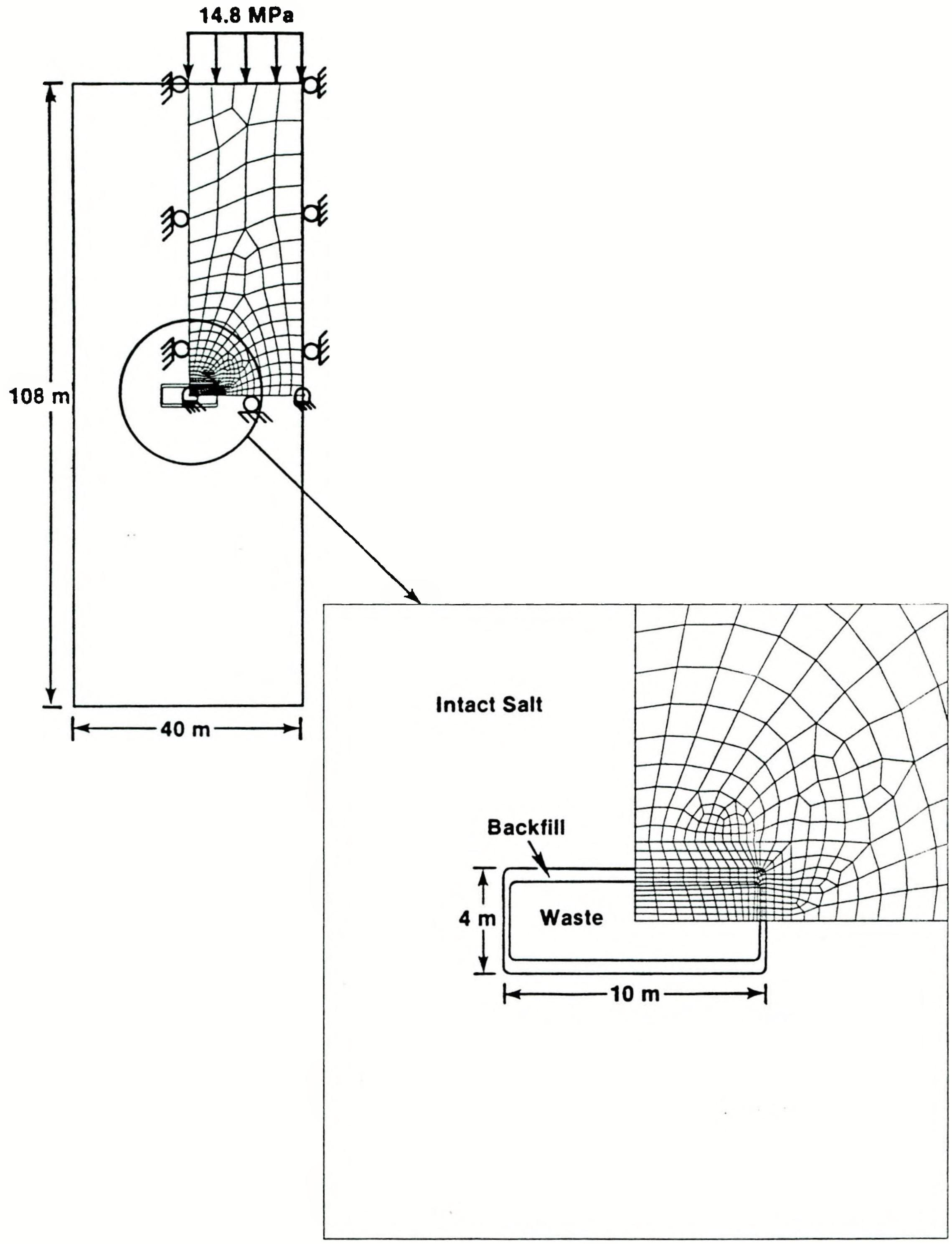

Figure 1: Finite element model of the disposal room.

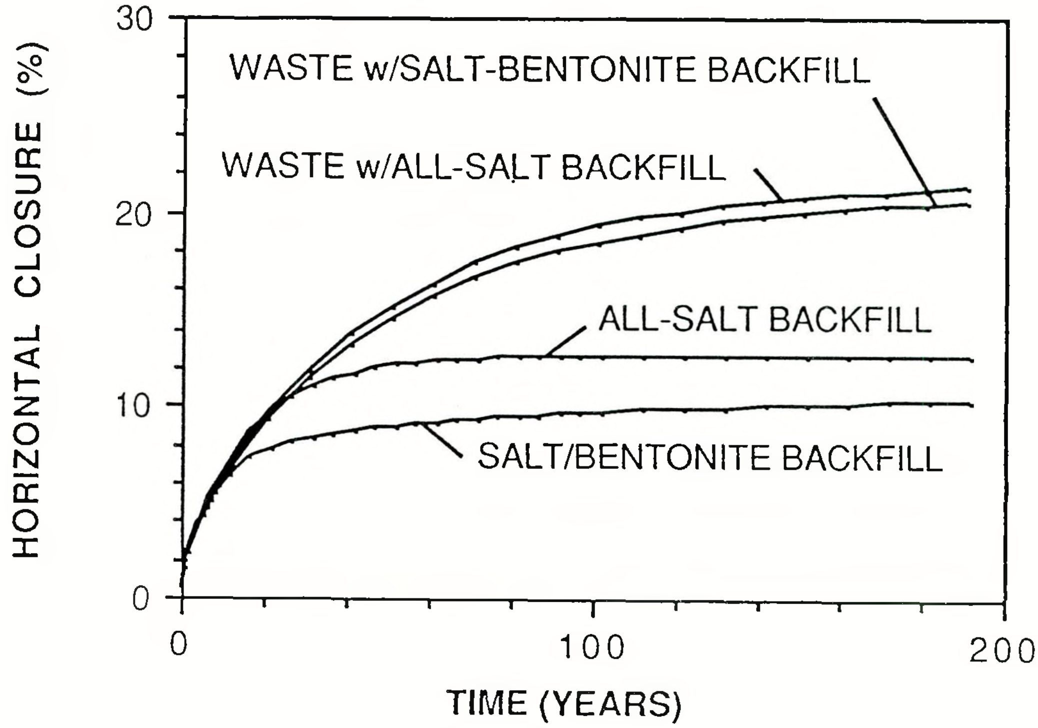

Figure 2: Horizontal closure of the disposal room as a function of time. The closure is measured at the midheight of the rib, and is expressed as a percentage of the initial width of the room.

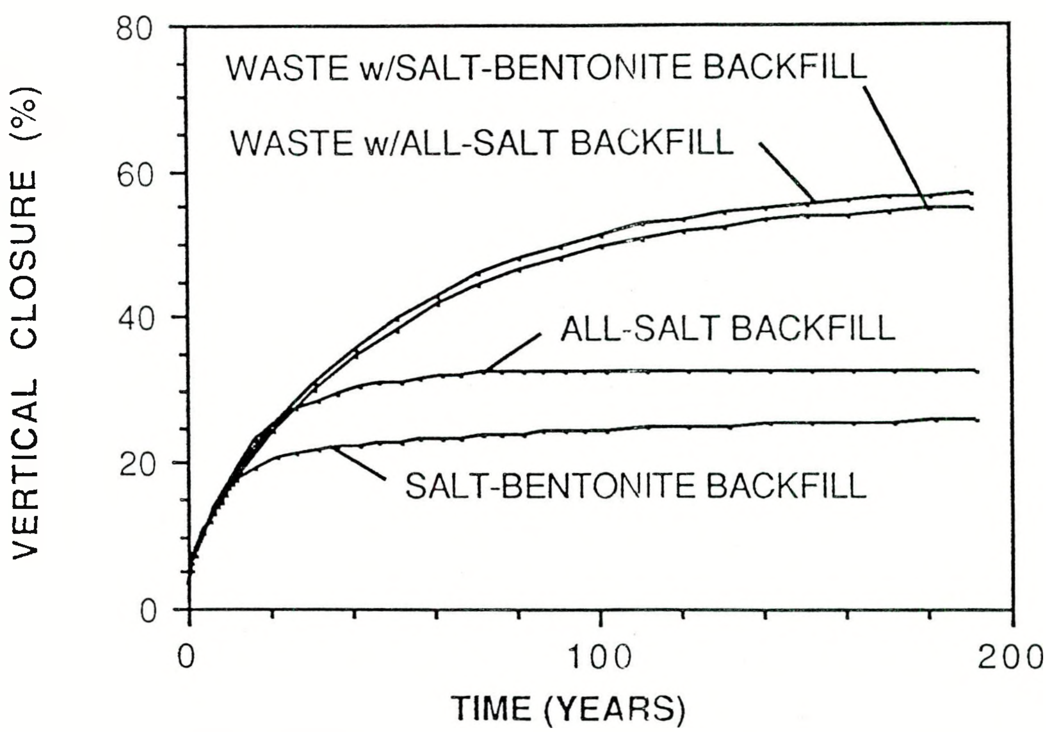

Figure 3: Vertical closure of the disposal room as a function of time. The closure is measured at the center of the roof and floor, and is expressed as a percentage of the initial height of the room.

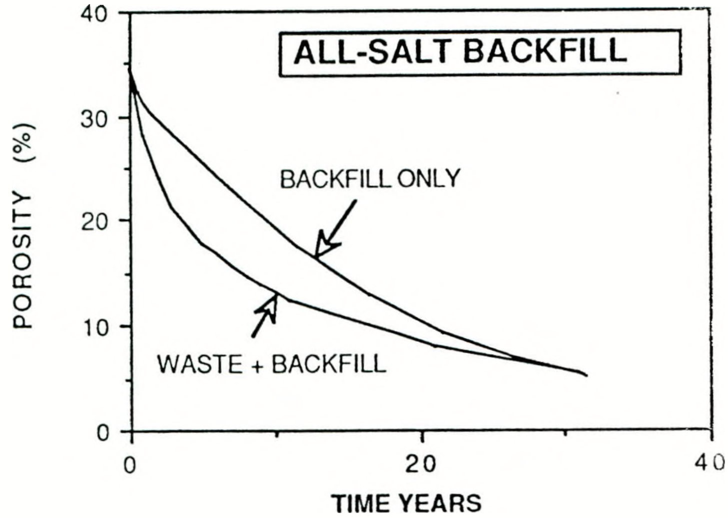

Figure 4: Average porosity in the backfilled region for the two cases with all-salt backfill.

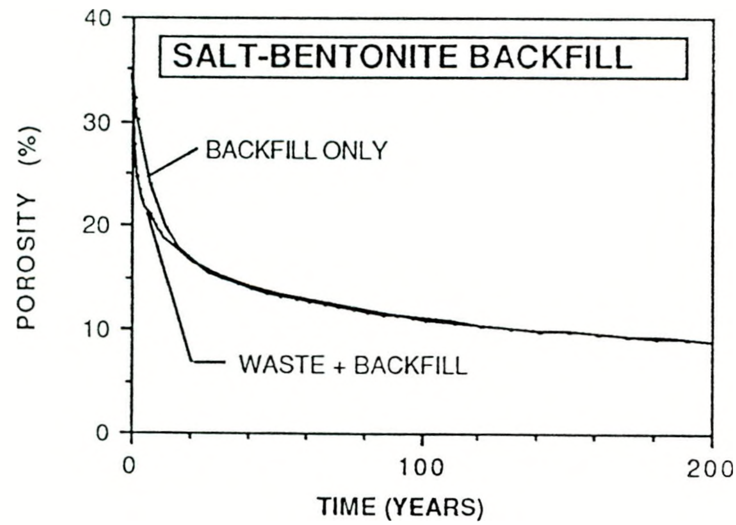

Figure 5: Average porosity in the backfilled region for the two cases with salt-bentonite backfill.

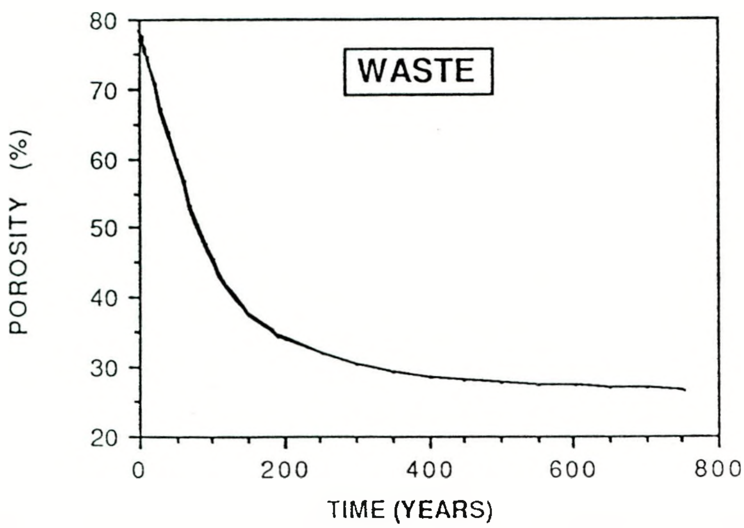

Figure 6: Average porosity in the waste region for the two cases with waste.